Mon. Not. R. Astron. Soc. **000**, 1–?? (2015) Printed 5 April 2016 (MN LATEX style file v2.2)

A note on periodicity of long-term variations of optical continuum in active galactic nuclei

Kai-Xing Lu[1,2⋆], Yan-Rong Li[2], Shao-Lan Bi[1] and Jian-Min Wang[2,3,*†]
[1]*Department of Astronomy, Beijing Normal University, Beijing 100875, China*
[2]*Key Laboratory for Particle Astrophysics, Institute of High Energy Physics (IHEP), Chinese Academy of Sciences, 19B Yuquan Road, Beijing 100049, China*
[3]*National Astronomical Observatories of China, Chinese Academy of Sciences, 20A Datun Road, Beijing 100020, China*

arXiv:1604.00587v1 [astro-ph.GA] 3 Apr 2016

Accepted 2016 April 01. Received 2016 April 01; in original form 2015 November 15

ABSTRACT
Graham et al. found a sample of active galactic nuclei (AGNs) and quasars from the Catalina Real-time Transient Survey (CRTS) that have long-term periodic variations in optical continuum, the nature of the periodicity remains uncertain. We investigate the periodic variability characteristics of the sample by testing the relations of the observed variability periods with AGN optical luminosity, black hole mass and accretion rates, and find no significant correlations. We also test the observed periods in several different aspects related to accretion disks surrounding single black holes, such as the Keplerian rotational periods of 5100 Å photon-emission regions and self-gravity dominated regions and the precessing period of warped disks. These tests shed new lights on understanding AGN variability in general. Under the assumption that the periodic behavior is associated with SMBHB systems in particular, we compare the separations ($\mathscr{D}_\bullet$) against characteristic radii of broad-line regions ($R_{\rm BLR}$) of the binaries and find $\mathscr{D}_\bullet \approx 0.05R_{\rm BLR}$. This interestingly implies that these binaries have only circumbinary BLRs.

Key words: galaxies: active – galaxies: nuclei – galaxies: evolution

1 INTRODUCTION

The optical and ultraviolet spectra of AGNs and quasars have been understood profoundly since their discovery. Accretion onto supermassive black holes (SMBHs) located in galactic centres is powering the giant emissions of AGNs and quasars through release of gravitational energy of the infalling gas (Rees 1984). It is well understood that the broad emission lines arise from gas photoionized by accretion disks of SMBHs (Osterbrock & Mathews 1986). According to the hypothesis of supermassive black hole binaries (SMBHBs; Begelman et al. 1980), there should be some AGNs and quasars powered by them at least (Gaskell 1983), manifesting with double-peaked or asymmetric emission lines (Shen & Loeb 2010) and long-term periodic variations (Runnoe et al. 2015). Although there are indeed growing indirect evidence for SMBHBs (e.g., Yan et al. 2015 based on special characteristic of spectral energy distributions, or Liu et al. 2014 on features of tidal disruption event in galactic centres), identification of them, in particular in sub-parsec scale, is still challenging.

Since long-term monitoring campaigns are extremely time-consuming, only a few AGNs and quasars, such as OJ 287 (Valtonen et al. 2008), PG 1302-102 (Graham et al. 2015a) and PSO J334.2028+01.4075 (Liu et al. 2015), have been found to exhibit long-term periodic (or quasi) variations of a few to ~ 10 years in optical and ultraviolet continuum. A major advance was made recently by Graham et al. (2015b, hereafter G15b), who performed a systematic search for the long-term periodical variations of continuum in quasars covered by the CRTS and finally identified more than one hundred of candidates. Periodic variability is generally believed to be a common signature of SMBHBs, but there also exist alternative explanations (Graham et al. 2015a; Li et al. 2016; G15b). The CRTS sample offers an opportunity to test the periodicity and probe the properties of SMBHBs. In this paper, we extend the G15b study to show more statistics of the long-term periodicity. Throughout this work, we assume a standard ΛCDM cosmology with $H_0 = 67\ {\rm km\ s^{-1}\ Mpc^{-1}}$, $\Omega_\Lambda = 0.68$ and $\Omega_{\rm M} = 0.32$ (Ade et al. 2014).

2 THE SAMPLE

The CRTS sample consists of 111 quasars with unambiguous observed periods from a few to ~ 5 years, as listed in Table 1 of G15b. We cross-checked the sample with Sloan Digital Sky Survey (SDSS) data and found available spectra for 90 quasars. Data Reduction of the SDSS spectra followed the procedures described in Hu et al. (2008). We measured the 5100 Å luminosity and full

⋆ E-mail: lukx@mail.bnu.edu.cn
† E-mail: wangjm@mail.ihep.ac.cn

© 2015 RAS

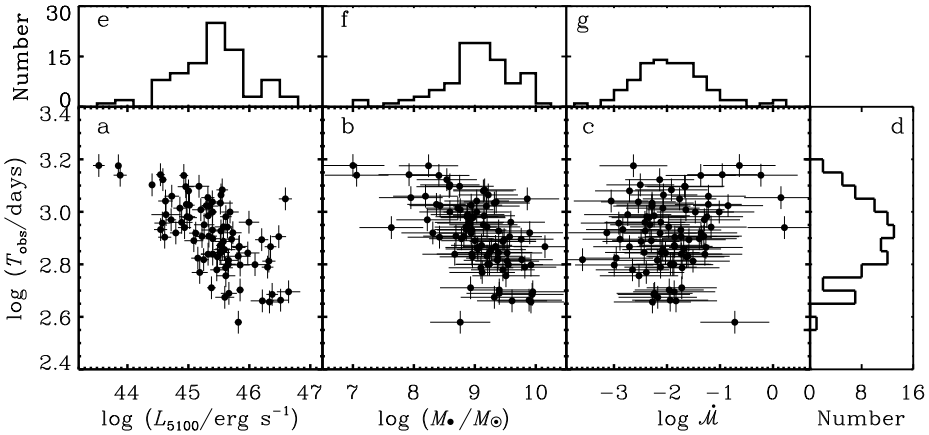

Figure 1. The observed $T_{\rm obs}$ in rest-frame versus luminosity (L_{5100}), black hole mass ($M_\bullet$) and accretion rates ($\dot{\mathscr{M}}$) in panels (*a, b, c*). The apparent correlations are spurious and caused by the redshift effect (see Section 3.1 for details), panels (*d, e, f, g*) is the distribution of ($T_{\rm obs}$, L_{5100}, $M_\bullet$, $\dot{\mathscr{M}}$)

width at half maximum (FWHM) of the broad Hβ and Mg II lines. We used a relation of $L_{5100} = 0.56 L_{3000}$ to convert the ultraviolet continuum into 5100 Å (Shen et al. 2008).

We used the well-established relation between BLR size and AGN 5100 Å luminosity ($R - L$ relation; Bentz et al. 2013) to estimate the BLR size

$$R_{\rm BLR} \approx 36.3\, \ell_{44}^{0.54}\ {\rm ltd}, \tag{1}$$

where $\ell_{44} = L_{5100}/10^{44}$ erg s^{-1} is the luminosity at 5100Å. We followed the standard way of estimating BH mass,

$$M_\bullet = f_{\rm BLR} \frac{V_{\rm FWHM}^2 R_{\rm BLR}}{G} = 5.27\times10^7\ f_{\rm BLR} V_{3000}^2 R_{30}\ M_\odot, \tag{2}$$

where G is the gravitational constant, $R_{30} = R_{\rm BLR}/30$ lt-d, $V_{3000} = V_{\rm FWHM}/3000$ km s^{-1} is the FWHM velocity, and $f_{\rm BLR}$ is a constant which includes all the unknown information about the geometry and kinematics of the BLR. The factor $f_{\rm BLR}$ is obtained by calibrating Equation (2) against SMBH mass obtained from the well known $M_\bullet - \sigma_*$ relationship in local bulge galaxies. We took $f_{\rm BLR} = 1.0$ in this paper (Ho & Kim 2014).

Note that Equation (2) only applies to local quasars with Hβ emission line ($z < 0.7$). For high$-z$ quasars, we used the extended relation of Equation (2) using Mg II emission line (Vestergaard & Peterson 2006). We then use the obtained black hole mass to calculate the parameters of accretion disks and extensively explore if the observed long-term periods are related to accretion disks (see §3 below).

In Table 1, we list the main properties of the sample. G15b determined the observed periods of the sample by the WWZ$-$ACF method, which gives a typical uncertainty of 10 percent for the periods. For the uncertainties of black hole mass estimate, we included the intrinsic scatters of 0.4 dex (Vestergaard & Peterson 2006). For the uncertainties of 5100 Å luminosity L_{5100}, we digitized the light curves from G15b (see their Figure 7) and included the standard deviation of light curves.

Figures 1(*e, f, g, h*) plot the distributions of the observed periods, 5100 Å luminosities, black hole mass and accretion rates (see §3 for a definition). The current sample shows that 1) the period peaks at ∼800 days; 2) the luminosity cover from $\sim 10^{44}$ erg s^{-1} to $\sim 10^{47}$ erg s^{-1}; 3) the black hole mass at $\sim 10^9 M_\odot$, but extends to $10^{10} M_\odot$; and 4) the accretion rate spans from $\sim 10^{-3}$ to 10^{-1}. The moderate accretion rates indicate that the objects of the sample are in the regime of standard accretion disk model, which is described by Shakura & Sunyaev (1973).

3 STATISTICS OF THE PERIODS

As for the accretion disks, we study four characteristic radii and explore if they can account for the long-term periodicity. In the standard accretion disk model, the effective temperature as a function of disk radius is given by

$$T_{\rm eff}(R) = \left(\frac{3GM_\bullet \dot{M}_\bullet}{8\pi R^3 \sigma_{\rm SB}}\right)^{1/4} \approx 3.32\times10^3\, \dot{\mathscr{M}}^{1/4} M_8^{-1/4} r_3^{-3/4}\ {\rm K}, \tag{3}$$

where $\sigma_{\rm SB}$ is the Stefan-Boltzman constant, $r_3 = R/10^3 R_{\rm g}$, $R_{\rm g} = 1.5\times10^{13} M_8$ cm is the gravitational radius, $\dot{\mathscr{M}} = \dot{M}_\bullet/L_{\rm Edd}c^{-2}$ is the dimensionless accretion rate, and $L_{\rm Edd} = 1.26\times10^{38}\,(M_\bullet/M_\odot)$ erg s^{-1} is the Eddington luminosity. Here we neglect the inner boundary condition. The emergent spectra of accretion disks are given by $L_\lambda \propto \int_{R_{\rm in}}^{\infty} B_\lambda(T_{\rm eff}) R dR$, where $R_{\rm in}$ is the inner radius of the disk and $B_\lambda(T_{\rm eff})$ is the Planck function. This yields the well-known canonic spectra as $L_\lambda \propto \lambda^{-1/3}$. It is easy to show that the accretion rate can be expressed by 5100 Å luminosity and black hole mass (Du et al. 2014)

$$\dot{\mathscr{M}} = 0.201 \left(\frac{\ell_{44}}{\cos i}\right)^{3/2} M_8^{-2}, \tag{4}$$

where $\cos i$ is the cosine of the inclination angle of the disk. We take $\cos i = 0.75$, which corresponds to the opening angle of the dusty torus.

3.1 Correlations with $L_{5100}, M_\bullet$ and $\dot{\mathscr{M}}$

Figure 1 show the relation between the rest-frame periods with the 5100 Å luminosities, black hole mass and accretion rates, respectively; apparent correlations can be seen. However, we note that the sample selection is based on both the magnitude limit and the time span of the monitoring ($\sim$ 9 years). Since the redshift distribution of the sample spans a wide range of $z \sim 0-3$, the relations of the rest-frame periods with AGN parameters will be significantly distorted by the redshift effect. Specifically, high-z quasars have higher luminosities but smaller rest-frame periods, leading to spurious correlations. We employ partial correlation analysis (see

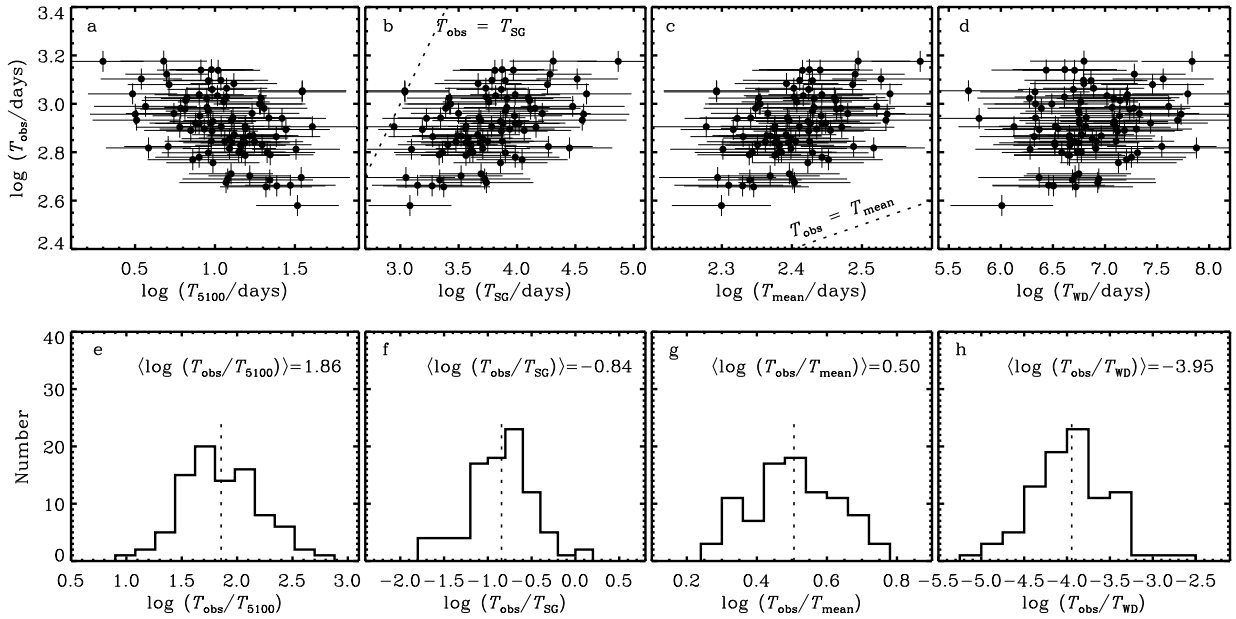

Figure 2. Comparison of observed periods in rest-frame versus the characteristic periods of accretion disks. Panels (*a*, *b*, *c*, *d*) is the Keplerian periods at the region for 5100Å photons (T_{5100}), the critical radius of self-gravity ($T_{\rm SG}$), averaged radius ($T_{\rm mean}$) and the precessing period of warped disks ($T_{\rm WD}$) versus observed periods($T_{\rm obs}$), respectively. Their corresponding histograms show in panels (*e*, *f*, *g*, *h*). Vertical dash lines are the average levels.

Table 1. The sample properties. Columns are the objects name, redshifts, optical luminosity, black hole mass, accretion rates, the radii of emitting 5100Å photons and BLR, and separations of the black hole binaries calculated from Kepler's law, respectively. (The full version is available in a machine-readable form in the online. A portion is shown here for guidance regarding its form and content.)

Object	z	$\log L_{5100}$ (erg s^{-1})	$\log(M_\bullet/M_\odot)$	$\log \dot{\mathscr{M}}$	$\log(R_{5100}/\mathrm{cm})$	$\log(R_{\rm BLR}/\mathrm{cm})$	$\log(\mathscr{D}_\bullet/\mathrm{cm})$
UM 234	0.729	45.35 ± 0.12	9.19 ± 0.55	-2.28 ± 0.73	15.16 ± 0.54	17.70 ± 0.21	16.54 ± 0.18
SDSS J014350.13+141453.0	1.438	45.65 ± 0.10	9.21 ± 0.53	-1.87 ± 0.71	15.31 ± 0.53	17.87 ± 0.20	16.40 ± 0.17
US 3204	0.954	45.39 ± 0.15	8.95 ± 0.57	-1.74 ± 0.76	15.19 ± 0.57	17.73 ± 0.24	16.40 ± 0.19
SDSS J072908.71+400836.6	0.074	43.53 ± 0.08	7.00 ± 0.52	-0.63 ± 0.68	14.25 ± 0.51	16.72 ± 0.18	15.92 ± 0.17

the Appendix) to quantitatively test if the correlations are caused by the redshift effect. The Spearman rank-order coefficients of the correlation between $\log T_{\rm obs}$ and ($\log L_{5100}$, $\log M_\bullet$, $\log \dot{\mathscr{M}}$) are $\boldsymbol{r} = (-0.64, -0.60, 0.14)$, respectively. The coefficients of the correlation between ($\log T_{\rm obs}$, $\log L_{5100}$, $\log M_\bullet$, $\log \dot{\mathscr{M}}$) and redshift are $\boldsymbol{r} = (-0.73, 0.81, 0.77, -0.16)$, respectively. The partial correlation coefficients between $\log T_{\rm obs}$ and ($\log L_{5100}$, $\log M_\bullet$, $\log \dot{\mathscr{M}}$) are $\boldsymbol{r} = (-0.10, -0.09, 0.03)$ with null probabilities of $p = (0.08, 0.10, 0.20)$, respectively. The low values of the partial correlation coefficients confirm that the apparent correlations are spurious. There are no significant correlation between the rest-frame period and optical luminosity, black hole mass and accretion rate.

If the periodicity arises from accretion disks of single black holes, the observed variability period and our correlation analysis provide useful restraints on variablitiy models in accretion disks. For example, Clarke & Shields (1989) propsoed a theoretical model based on disk thermal instability and predicted that the continuum variations of AGN obey a relation of $P \propto L^{1/2}$, and the timescale > 100 years for the high-luminosity AGNs, which is much longer than the observed periods of G15b sample.

On the other hand, under the SMBHB hypothesis, one may expect that the orbital period would depend on the total black hole mass of the system. However, partial correlation analysis shown that there is no correlation between the period ($T_{\rm obs}$ in rest-frame) and measured black hole mass. The intrinsic scatter of black hole mass estimated from the $R - L_{5100}$ relation is as large as 0.43 dex (e.g., Vestergaard & Peterson 2006). Meanwhile, the possible biases between measured black hole mass and "true" mass may lead to additional scatters (e.g., Shen et al. 2008). It is plausible that the intrinsic correlation between the periods and black hole mass is smeared out due to the large scatter of mass measurements.

3.2 Characteristic periods of accretion disks surrounding single black holes

We now turn to calculate the following four characteristic periods of accretion disks surrounding single black holes to test if they can account for the observed periods.

For the standard accretion disk model, the photons with a wavelength λ mainly come from the region with a temperature of $T_{\rm eff} = 2.37 \times 10^8/\lambda(\text{Å})$ K (Siemiginowska & Czerny 1989). We thus have the region for 5100 Å photons $R_{5100}/R_{\rm g} =$

$29.7\dot{\mathscr{M}}^{1/3}M_8^{-1/3}\lambda_{5100}^{4/3}$ from Equation (4), namely,

$$\frac{R_{5100}}{R_{\rm g}} = 17.4\left(\frac{\ell_{44}}{\cos i}\right)^{1/2} M_8^{-1}\lambda_{5100}^{4/3}, \quad (5)$$

where $\lambda_{5100} = \lambda/5100\text{Å}$.

The outer part of accretion disks are optically thick and geometrically thin, dominated by gas pressure. In a pioneering paper, Paczynski (1978) realized that this region is so distant that it is strongly affected by the vertical self-gravity of the disk rather than the central black hole. The self-gravity of the disk is $2\pi G\Sigma$, while the vertical force of the gravity is given by $GM_\bullet R^{-2}(H/R)$. Using the mass density of the outer part of accretion disks (the region C solution in Shakura & Sunyaev 1973)

$$\rho = 4.38\times10^{-9}\,\alpha_{0.1}^{-7/10}\dot{\mathscr{M}}^{11/20}M_8^{-7/10}r_3^{-15/8}{\rm g\,cm^{-3}}, \quad (6)$$

we have the Toomre parameter, defined by the ratio of the vertical force of the central black hole to the disk's self-gravity, as

$$Q = \frac{M_\bullet}{4\pi\rho R^3} = 1.10\,\alpha_{0.1}^{7/10}M_8^{-13/10}\dot{\mathscr{M}}^{-11/20}r_3^{-9/8}, \quad (7)$$

where $\alpha_{0.1} = \alpha/0.1$. When $Q \lesssim 1$, the disks become self-gravity dominated. This yields a critical radius of self-gravity as

$$\frac{R_{\rm SG}}{R_{\rm g}} = 1.09\times10^3\,\alpha_{0.1}^{28/45}M_8^{-52/45}\dot{\mathscr{M}}^{-22/45}. \quad (8)$$

With two radii of Equation (5) and (8), the corresponding Keplerian periods are given by

$$T_{5100,{\rm SG}} = 2\pi\sqrt{\frac{(R_{5100},R_{\rm SG})^3}{GM_\bullet}}, \quad (9)$$

where the subscripts refer to the corresponding radii. In addition, to account for the region between R_{5100} and $R_{\rm SG}$, we define an averaged radius as $\langle R\rangle = \sqrt{R_{5100}R_{\rm SG}}$ and the averaged period as

$$\langle T\rangle = 2\pi\sqrt{\frac{\langle R\rangle^3}{GM_\bullet}}. \quad (10)$$

At last, we can also calculate the characteristic period for warped disks. According to Shakura & Sunyaev (1973), the total mass of the disk within $R_{\rm SG}$ is

$$M_{\rm disk} \approx 2\pi R_{\rm SG}^2\,\Sigma_{\rm SG} \approx 1.42\times10^5\,\alpha_{0.1}^{-1/45}\ell_{44}^{6/45}M_8^{26/45}\,M_\odot, \quad (11)$$

where $\Sigma_{\rm SG}$ is the surface density of the disk at $R_{\rm SG}$. The warped disks precess with a typical period

$$T_{\rm WD} = 2\pi\sqrt{\frac{M_\bullet R_{\rm WD}^3}{GM_{\rm disk}^2}}, \quad (12)$$

where $R_{\rm WD}$ is typical radius ($R_{\rm WD}$=$R_{\rm SG}$) of the warped disk (Ulubay-Siddiki et al. 2009).

Figure 2 compares the rest-frame $T_{\rm obs}$ with T_{5100}, $T_{\rm SG}$, $T_{\rm mean}$ and $T_{\rm WD}$ in the top panels, and plots their respective ratios in the bottom panels. We find that $T_{\rm obs}$ is much longer than T_{5100}, but shorter than $T_{\rm SG}$, namely $T_{5100} < T_{\rm obs} < T_{\rm SG}$. This motivates us to compare $T_{\rm obs}$ with the mean value of rotational periods between R_{5100} and $R_{\rm SG}$. As shown by Figure 2*g*, $T_{\rm obs}$ is greater than $T_{\rm mean}$, implying that $T_{\rm obs}$ is related to the region between $R_{\rm SG}$ and $\langle R\rangle$ if the observed periodicity arises from an accretion disk surrounding a single black hole. Figure 2*h* shows that $T_{\rm obs}$ is much shorter than the period of warped disks driven by the self-gravity torque, so that we can rule out this possibility for the periodicity.

In next section, under the assumption that the observed periods are associated with SMBHB systems, we discuss several possible processes for the periodicity and calculate the BLR sizes and separations of these SMBHB systems.

4 SMBHB MODELS

4.1 Periodicity explanations

As pointed out by G15b, there exist several plausible processes responsible for the periodicity.

(i) *A processing jet*. In the sample, by checking the radio band data from the catalog of VLA-FIRST survey (Chang et al. 2004), we found that only 13 candidates are radio-loud, indicating that the periodic variations in most candidates are not caused by a precessing jet.

(ii) *Quasi-periodic oscillation*. Abramowicz & Kluźniak (2001) suggested that high-frequency QPOs arise from some type of resonance mechanism. Zhou et al. (2010) showed that the observed time-scales (T) of high-frequency QPOs correlate with black hole mass following $T = 6.22\,M_\bullet/\,(10^9\,M_\odot)$ days. For G15b sample, the typical value ($T \sim 6.22$ days) is much shorter than observed period. On the other hand, as for low-frequency QPOs, Yan et al. (2013) showed that GRS 1915+105 has a mass of $\sim 12M_\odot$ and exhibits QPO with 1 Hz. If we assume that the period $T \propto M_\bullet$, the case of GRS 1915+105 would mean that the period if QPOs of G15b sample, spanning a mass range of $10^8 - 10^{10}M_\odot$, lies in a range between $\sim$ 100 to 10^4 days (in observed-frame). This is generally comparable with the range of observed periods in G15b sample.

(iii) *Periodic accretion*. The orbital motion of binaries induces periodic modulation of mass accretion onto each black hole (Farris et al. 2014), which translates into periodic emissions of the accretion disks. The issue about this explanation is that the viscous time of an accretion disk, which reflects the timescale of its response to a change in mass accretion rate, is generally much longer than the observed periods of the present sample.

(iv) *Relativistic Doppler boosting*. Recently, D'Orazio et al. (2015) proposed an alternative explanation for the periodicity by relativistic Doppler boosting and applied it to the periodic light curve of PG 1302-102. In this model, a large inclination of the binary's orbit is generally required to account for the variation amplitude. This will rise a concern about the obscuration of the outer dusty torus if the dusty torus is coplanar with the binary's orbit.

(v) *Warped accretion disk*. The accretion disks are warped due to tidal torques if their spin axis is misaligned with the orbital axis of the binaries. The warps precess along with the binary's orbital motion and eclipse some parts of the disk emissions, leading to periodic variations in the disk emissions.

In a nutshell, we can only generally exclude with certainty the possibility of the precessing jet model and high-frequency QPOs for the periodicity. For the other models, we need more observations, in particular spectroscopic data, to test them.

4.2 Separations and BLR sizes

Under the assumption that the periodicity arises from a SMBHB system, we now calculate the binary's separation, given with the observed period, and compare it against the BLR size predicted from the $R-L$ relation. Using the Kepler's law of $\mathscr{D}_\bullet = \left(GM_\bullet T_{\rm obs}^2/4\pi^2\right)^{1/3}$ and Equation (2), we have the binary's semi-major axis as

$$\mathscr{D}_\bullet = \left(\frac{f_{\rm BLR}}{4\pi^2}\right)^{1/3}\left(V_{\rm FWHM}^2T_{\rm obs}^2R_{\rm BLR}\right)^{1/3}. \quad (13)$$

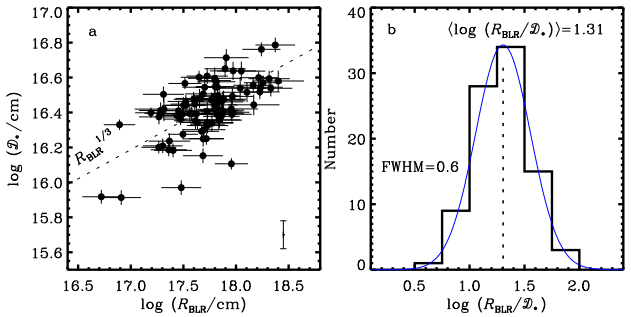

Figure 3. Comparison of SMBHB separations ($\mathscr{D}_\bullet$) with the sizes of broad-line regions ($R_{\rm BLR}$) in panels (*a*, *b*). In panel (*a*), dotted line is the expected relation. The bar plotted in the right lower corner represents the typical scatters of $\mathscr{D}_\bullet$. In panel (*b*), blue line is the Gaussian fit to the distribution.

This indicates $\mathscr{D}_\bullet \propto R_{\rm BLR}^{1/3}$ for given $V_{\rm FWHM}$ and $T_{\rm obs}$ (Figure 3*a*). We can also rewrite Equation (13) into

$$\frac{\mathscr{D}_\bullet}{R_{\rm BLR}} = 0.07\, f_{\rm BLR}^{1/3} V_{3000}^{2/3} T_1^{2/3} R_{30}^{-2/3}, \qquad (14)$$

where $T_1 = T_{\rm obs}/{\rm year}$. Figure 3*b* shows that $\mathscr{D}_\bullet$ is smaller than $R_{\rm BLR}$ and in average, $\mathscr{D}_\bullet \approx 0.05 R_{\rm BLR}$ in the sample. The FWHM of the $\log(R_{\rm BLR}/\mathscr{D}_\bullet)$ distribution is 0.6. This interestingly means that the BLRs of the binary have been merged, but the binary black holes are still co-rotating.

5 CONCLUSIONS

We have tested the periodicity of long-term optical variations in a sample of AGNs from G15b. The partial correlation analysis shows that the observed periods of G15b sample are uncorrelated with the AGN 5100 Å luminosity, (total) black hole mass and accretion rates. By comparing the observed periods with the characteristic periods of accretion disks surrounding single black holes, we found that the periods generally lies within the Keplerian periods that correspond to the regions between the 5100 Å region and the self-gravity radius. We discussed several existing explanations for the periodicity in the context of SMBHB hypothesis and concluded that further observations (particularly long-term spectroscopic monitoring) are required to test if the periodicity originate from SMBHB systems (e.g., Li et al. 2016). Nevertheless, by assuming that observed periodicity is associated with SMBHB systems, we calculated the SMBHB's separations and found that they are smaller than the sizes of broad-line regions, implying that the binary BLRs have been merged.

ACKNOWLEDGEMENTS

We are grateful to the referee for constructive suggestions that significantly improved the manuscript. We thank the IHEP AGN members for useful discussions. This research is supported by NSFC-11173023, -11133006, -11233003, -11273007 and -11573026.

APPENDIX A: PARTIAL CORRELATION ANALYSIS

For the parameter sets $(\boldsymbol{x_i}, \boldsymbol{y_i}, \boldsymbol{z_i})$, $i = 1, 2..., N$. The correlation coefficient between $\boldsymbol{x}$ and $\boldsymbol{y}$ excluding the dependence on the third parameter of $\boldsymbol{z}$ is evaluated as (e.g., Kendall & Stuart 1979)

$$\boldsymbol{r}_{xy,z} = \frac{\boldsymbol{r}_{xy} - \boldsymbol{r}_{xz}\boldsymbol{r}_{yz}}{\sqrt{1-\boldsymbol{r}_{xz}^2}\sqrt{1-\boldsymbol{r}_{yz}^2}}, \qquad (A1)$$

where $\boldsymbol{r}_{xy}$, $\boldsymbol{r}_{xz}$ and $\boldsymbol{r}_{yz}$ is the Spearman rank-order correlation coefficient between $\boldsymbol{x}$ and $\boldsymbol{y}$, between $\boldsymbol{x}$ and $\boldsymbol{z}$ and between $\boldsymbol{y}$ and $\boldsymbol{z}$, respectively (Press et al. 1992). $\boldsymbol{r}_{xy,z}$ is partial correlation coefficients.

REFERENCES

Abramowicz, M. A., & Kluźniak, W. 2001, A&A, 374, L19
Ade, P. A. R., Arnaud, M., et al. 2014, A&A, 571, A31
Begelman, M. C., Blandford, R. D., & Rees, M. J. 1980, Nature, 287, 307
Bentz, M. C., Denney, K. D., Grier, C. J., et al. 2013, ApJ, 767, 149
Chang, T.-C., Refregier, A., & Helfand, D. J. 2004, ApJ, 617, 794
Clarke, C. J., & Shields, G. A. 1989, ApJ, 338, 32
Du, P., Hu, C., Lu, K.-X., et al. 2014, ApJ, 782, 45
D'Orazio, D. J., Haiman, Z., & Schiminovich, D. 2015, Nature, 525, 351
Farris, B. D., Duffell, P., MacFadyen, A. I., & Haiman, Z. 2014, ApJ, 783, 134
Gaskell, C. M. 1983, Liege International Astrophysical Colloquia, 24, 473
Graham, M. J., Djorgovski, S. G., Stern, D., et al. 2015a, Nature, 518, 74
Graham, M. J., Djorgovski, S. G., Stern, D. et al. 2015b, MNRAS, 453, 1562
Ho, L. C., & Kim, M. 2014, ApJ, 789, 17
Hu, C., Wang, J.-M., Ho, L. C., et al. 2008, ApJ, 687, 78
Kendall, M., & Stuart, A. 1979, London: Griffin, 1979, 4th ed.,
Li, Y.-R., Wang, J.-M., Ho, L. C., et al. 2016, ApJ in press (arXiv:1602.05005)
Liu, T., Gezari, S., Heinis, S., et al. 2015, ApJ Letters, 803, L16
Liu, F. K., Li, S., & Komossa, S. 2014, ApJ, 786, 103
Osterbrock, D. E., & Mathews, W. G. 1986, ARA&A, 24, 171
Paczyński, B. 1978, AcA, 28, 91
Press, W. H., Teukolsky, S. A., Vetterling, W. T., & Flannery, B. P. 1992, Cambridge: University Press, —c1992, 2nd ed.,
Rees, M. J. 1984, ARA&A, 22, 471
Runnoe, J. C., Eracleous, M., Mathes, G., et al. 2015, ApJS, 221, 7
Shakura, N. I., & Sunyaev, R. A. 1973, A&A, 24, 337
Shen Y., Greene J. E., Strauss M. A., Richards G. T., Schneider D. P., 2008, ApJ, 680, 169-190
Shen, Y., & Loeb, A. 2010, ApJ, 725, 249
Siemiginowska, A., & Czerny, B. 1989, MNRAS, 239, 289
Ulubay-Siddiki, A., Gerhard, O., & Arnaboldi, M. 2009, MNRAS, 398, 535
Valtonen, M. J., Lehto, H. J., Nilsson, K., et al. 2008, Nature, 452, 851
Vestergaard, M., & Peterson, B. M. 2006, ApJ, 641, 689
Yan, C.-S., Lu, Y., Dai, X., & Yu, Q. 2015, ApJ, 809, 117
Yan, S.-P., Ding, G.-Q., Wang, N., Qu, J.-L., & Song, L.-M. 2013, MNRAS, 434, 59
Zhou, X.-L., Zhang, S.-N., Wang, D.-X., & Zhu, L. 2010, ApJ, 710, 16